AIS is an oncogene amplified in squamous cell carcinoma

Kenji Hibi*†, Barry Trink*†, Meera Patturajan*, William H. Westra*‡, Otávia L. Caballero*, David E. Hill§, Edward A. Ratovitski*, Jin Jen*, and David Sidransky*¶

*Department of Otolaryngology–Head and Neck Surgery, Division of Head and Neck Cancer Research, and ‡Department of Pathology, Johns Hopkins University School of Medicine, 818 Ross Research Building, 720 Rutland Avenue, Baltimore, MD 21205-2196; and §Oncogene Research Products, 84 Rogers Street, Cambridge, MA 02142

Communicated by Harry Rubin, University of California, Berkeley, CA, February 24, 2000 (received for review December 22, 1999)

We and others recently isolated a human *p53* homologue (*p40/p51/p63/p73L*) and localized the gene to the distal long arm of chromosome 3. Here we sought to examine the role of *p40/p73L*, two variants lacking the N-terminal transactivation domain, in cancer. Fluorescent *in situ* hybridization (FISH) analysis revealed frequent amplification of this gene locus in primary squamous cell carcinoma of the lung and head and neck cancer cell lines. (We named this locus *AIS* for amplified in squamous cell carcinoma.) Furthermore, amplification of the *AIS* locus was accompanied by RNA and protein overexpression of a variant p68^{AIS} lacking the terminal transactivation domain. Protein overexpression in primary lung tumors was limited to squamous cell carcinoma and tumors known to harbor a high frequency of *p53* mutations. Overexpression of p40^{AIS} in Rat 1a cells led to an increase in soft agar growth and tumor size in mice. Our results support the idea that *AIS* plays an oncogenic role in human cancer.

p63 tumor-suppressor gene

Alterations of the *p53* tumor-suppressor gene and its encoded protein are the most frequently encountered genetic events in human malignancy (1). It is now established that the p53 protein is central to the cellular response to a wide variety of stressful stimuli. These stimuli, which include DNA damage, hypoxia, heat shock, metabolic changes, and certain cytokines, activate the p53 protein, which in turn drives a series of events that culminate in cell cycle arrest or apoptosis (2, 3).

The importance of p53 in both normal homeostasis of a cell and tumorigenesis drove the search for homologues of p53. The *p53*-related gene *p73* (located on chromosomal arm 1p) was reported, showing strong sequence homology with various key regions of *p53* (4). However, despite its location within a tumor suppressor locus and its ability to mimic p53 in certain transcriptional and growth control assays, the role of *p73* in human cancers is still unclear. Unlike p53, p73 was induced only by cisplatin and not by other agents that induce damage (5). Moreover, the remaining allele in neuroblastomas that have undergone loss of heterozygosity was not inactivated (6).

Using degenerate PCR primers based on conserved regions in the DNA-binding domains of p53 and p73, we cloned an additional member of this family, *p40* (7). Concurrently, other groups cloned different isoforms of the same gene and referred to their products as p51, p63, and p73L (8–10). The main difference between the various transcripts is the presence or absence of the N-terminal transcriptional activation (TA) domain; p40, ΔNp63, and p73L lack this domain.

One alternative transcript containing a TA domain (p51) was shown to suppress colony formation and to transcriptionally activate *p21* in a fashion similar to the *p53* tumor suppressor gene (8). However, a transcript lacking the N-terminal transactivation domain was found to act in a dominant-negative fashion and was able to suppress p53 transactivation (9).

We found no evidence of a tumor suppressor function for the *p40/p51/p63/p73L* gene. Instead, we observed overexpression of this gene in head and neck cancer cell lines and primary lung cancers associated with a low increase of its copy number. Because this gene is amplified in squamous cell carcinoma, we now refer to it as *AIS*. Moreover, because multiple products of the *AIS* gene share the central core domain (p40^{AIS}), we used this protein in functional studies. In transformation assays, Rat 1a cells with *p40*^{AIS} expression developed larger colonies in soft agar and bigger tumors in nude mice compared with cells with an empty vector. Our data thus support the concept that AIS transcripts lacking the TA domain may play an oncogenic rather than a suppressive role in certain cancers.

Materials and Methods

Tumor Source and Cell Lines. Primary tumors were collected from patients diagnosed with head and neck carcinoma or lung carcinoma between the years 1993 and 1999 at The Johns Hopkins University. Fresh tumors were obtained from surgical resection and stored at −80°C for DNA and RNA analysis. Paraffin blocks were made available from the department of pathology for immunohistochemical analysis. All cell lines were isolated in the Department of Otolaryngology at The Johns Hopkins University (1985–1992) with the exception of SaOs2, FaDu, and HEK293, which were obtained from the American Type Culture Collection.

Mutation Analysis. The PCR amplification of tumor cDNA samples consisted of 35 cycles at 95°C for 1 min, 55°C for 1 min, 72°C for 1 min. The primers used for *p40* amplification were S1 (sense), 5′-GCAGCATTGATCAATCTTACAG and AS2 (antisense), 5′-TGAATTCACGGCTCAGCTCAT; S3 (sense), 5′-CGCCATGCCTGTCTACAAAAA and AS4 (antisense), 5′-GCCTCCTAAAATGACACGTTG. All PCR products were purified and sequenced directly with the AmpliCycle sequencing kit (Perkin–Elmer). The sequencing primers were 5′-GCCACAGTACACGAACCTGG, 5′-AAAAGCTGAGCACGTCACGG, 5′-CTTCACCACCTCCGTGACGT, 5′-AGGTTGGCACTGAATTCACGA, 5′-AAAATTGGACGGCGGTTCAT, 5′-GTGATGGTACGAAGCGCCC, and 5′-ACGGGCGCTTCGTACCAT. Mutation analysis for the *p53* gene was performed as described previously (11).

AIS Adenovirus. A full-length p40^{AIS} cDNA was cloned from a human prostate cDNA library as previously described (7). The

Abbreviations: TA domain, transcriptional activation domain; FISH, fluorescent *in situ* hybridization; HNSCC, head and neck squamous cell carcinoma; RT-PCR, reverse transcription–PCR.

†K.H. and B.T. contributed equally to this work.

¶To whom reprint requests should be addressed at: Department of Otolaryngology–Head and Neck Surgery, Division of Head and Neck Cancer Research, Johns Hopkins University School of Medicine, 818 Ross Research Building, 720 Rutland Avenue, Baltimore, MD 21205-2196. E-mail: dsidrans@jhmi.edu.

The publication costs of this article were defrayed in part by page charge payment. This article must therefore be hereby marked "*advertisement*" in accordance with 18 U.S.C. §1734 solely to indicate this fact.

construct was then subcloned into the shuttle vector, pAdTrack-CMV. The resultant plasmid was linearized by digesting with the restriction endonuclease *Pme*I, and subsequently cotransformed into *Escherichia coli* BJ5183 cells with an adenoviral backbone plasmid, pAdEasy-1. Recombinants were selected for kanamycin resistance, and recombination was confirmed by restriction digest analysis. The linearized recombinant plasmid was then transfected into the adenovirus packaging cell line, HEK-293, which was described in detail previously (12).

Northern Analysis. For primary tissues, the collected samples were grossly dissected and quickly frozen or lysed immediately in the guanidine buffer, and the RNA was isolated by using a CsCl gradient method. For cancer cell lines, total RNA was isolated by using the Trizol reagent (GIBCO/BRL). Northern blot hybridization using the cDNA probes was performed as described (13).

Fluorescent *in Situ* Hybridization (FISH) Analysis. FISH was performed as previously described (14). Specifically, 4-μm-thick sections were cut out and mounted on glass slides, fixed in a methanol and glacial acetic acid (3:1) solution for 5 min, and then dehydrated in ethanol series and allowed to air dry. Cell lines were fixed in the same fixative described above and dropped onto glass slides. Samples were denatured in 70% formamide and 2× SSC at 75°C for 5 min, followed by dehydration in cold ethanol. The bacterial artificial chromosome (BAC) probe containing *AIS* was isolated as described (7) and was labeled by nick translation with digoxigenin-11-dUTP (Boehringer Mannheim), and the biotin-labeled centromere probe for chromosome 3 was purchased from Vysis (Downers Grove, IL). The hybridization mixture consisted of 10% dextran sulfate, 50% formamide, 2× SSC, 0.1 μg of the labeled probe, 10 μg of Cot-1 DNA (GIBCO/BRL), and 10 μg of salmon sperm DNA. Before hybridization, the mixture was denatured at 75°C for 5 min and then incubated at 37°C for 15 min. The probes were hybridized overnight to denatured tissue sections at 37°C. After hybridization, slides were washed for 5 min with 0.5× SSC at 72°C and then incubated with rhodamine-anti-digoxigenin and FITC-avidin (Oncor). The samples were counterstained with 2-phenylindole·dihydrochloride and examined under a Zeiss Axiophot epifluorescence microscope. Tumor areas were determined by evaluating the hematoxylin- and eosin-stained adjacent sections. Up to 200 nuclei per slide signals were counted under a double-band pass filter. The number of AIS and chromosome 3 signals was counted for each nucleus. When the AIS-to-chromosome 3 ratio was less than 1, we defined it as not amplified. When it was more than 1, we defined it as a relative amplification of AIS. FISH on normal specimens or nonmalignant areas was analyzed in the same manner as a control. For documentation, images were captured by a charge-coupled device camera (Photometrics, Tucson, AZ) and processed by using the Oncor Image analyzing system.

Immunohistochemistry. Sections 6 μm thick were made from paraffin tissue blocks and the slides were dried at 60°C for 30 min, treated with xylenes, and then dehydrated in alcohol. Endogenous peroxidase was blocked with 0.3% H_2O_2. After blocking with normal goat serum, the slides were incubated with the polyclonal rabbit antiserum against AIS at 1:2000 dilution for 1 h at room temperature. A polyclonal antibody was made against a specific peptide (residues 5–17, ENNAQTQFSEPQY); this antibody recognizes the AIS isoforms without the TA domain. A Vectastain ABC Kit and DAB Substrate Kit (Vector Laboratories) were used to visualize the antibody binding.

Immunohistochemical analysis for AIS protein was interpreted to determine AIS-positive and -negative staining. Only nuclear staining was interpreted as positive. For control studies, head and neck squamous cell carcinoma (HNSCC) cell line 022 and lung cancer cell line H1299 were used as positive and negative controls, respectively. The AIS status of these two cell lines was confirmed by Northern analysis. Optimized conditions were then used for the immunostaining of primary lung cancer specimens. For confirmation of the specificity of the anti-AIS antibody, we performed Western analysis using SaOs2 [negative for all AIS transcripts by reverse transcription (RT)-PCR], $p40^{AIS}$ adenovirus-infected SaOs2, and an HNSCC cell line (022). We identified a specific band in each positive control cell lysate with the AIS antibody, whereas no bands were detected with preimmune serum. Unless stated otherwise, this polyclonal antibody (Oncogene Research Products, Cambridge, MA) was used in all protein studies.

Western Analysis. Cells from a T-75 flask were trypsinized and washed with phosphate-buffered saline (PBS) and suspended in 200 μl of RIPA buffer (50 mM Tris·HCl, pH 7.5/150 mM NaC1/1% Nonidet P-40/0.5% sodium deoxycholate/0.1% SDS) containing 1 mM PMSF. The lysate was incubated on ice for 20 min, followed by sonication for 5 sec and further incubated for another 20 min on ice. The lysate was then centrifuged at 10,000 rpm in a microcentrifuge for 10 min and supernatant was saved at −80°C. Proteins in 100-μg samples of cell lysates were separated on an SDS 10% polyacrylamide gel and transferred to a poly(vinylidene difluoride) (PVDF) membrane (Micron Separations, Westboro, MA) or a nitrocellulose membrane (Sartorius). After the nonspecific sites had been blocked by incubation in PBS + 5% nonfat dry milk, the blot was incubated with the polyclonal anti-AIS antibody at 1:2000 dilution for 1 h at room temperature. To identify the various AIS isoforms in HNSCC cell lines, we used commercial antibodies to p63 (N-18, 8C-8369), p63γ (R-20, SC-7255), and p63α (C-18, SC-8370) from Santa Cruz Biotechnology. After washing, an ECL kit (Amersham) was used to visualize the antibody binding to each protein. The PVDF membrane was then washed to get rid of attached antibody and reacted with antibody against actin (Chemicon) as an internal control.

Transfection Assay. A full-length $p40^{AIS}$ cDNA was cloned into pCEP4 (Invitrogen). pCEP4-$p40^{AIS}$ and pCEP4 were transfected into Rat 1a fibroblast cells by using Lipofectamine (GIBCO/BRL) according to the protocol provided by the manufacturer. Cells were selected with hygromycin B at 200 μg/ml, and $p40^{AIS}$ expression in Rat 1a-$p40^{AIS}$ cells was confirmed by immunohistochemistry.

Tumorigenicity Assay. For soft agar analysis, 10^5 cells of either Rat 1a-$p40^{AIS}$ or Rat 1a-no (vector only control) in 2-fold-concentrated DMEM/20% FBS were mixed with an equal volume of 0.8% agarose and poured onto a bed of 0.7% agarose. After 18 days, colonies were counted and measured under the microscope. All experiments were performed in triplicate, and differences were analyzed by the *t* test.

Tumor growth in nude mice was assayed by inoculating 5×10^6 cells of either Rat 1a-$p40^{AIS}$ or Rat 1a-no into the right or left flank, respectively, of five nude mice. At 21 and 24 days after inoculation, tumor size was measured in three dimensions. Differences in tumor volumes were analyzed by the *t* test.

Results

We and others recently described several splice variants of a *p53* homologue (*AIS*) on chromosome 3q as shown in Fig. 1 (7–10). We first examined *AIS* for mutations by using cDNA prepared by RT-PCR from 14 primary lung cancers and 6 HNSCC cell lines (Table 1). Two missense variants were observed. These changes involved codon 298 (Lys to Arg) in a primary lung cancer and codon 14 (Glu to Gln) in an HNSCC. Although paired

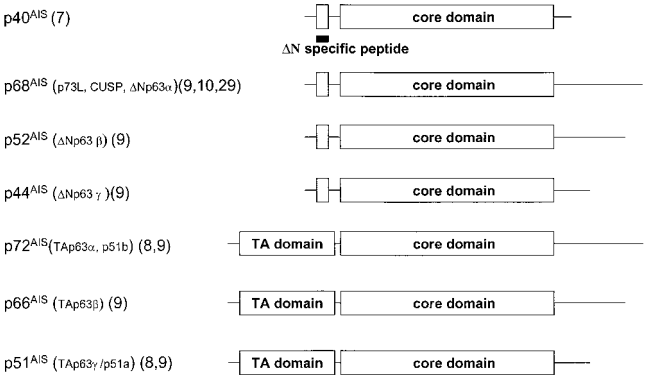

Fig. 1. The recent cloning of these variants by several groups (7–10, 29) has led to a potentially confusing nomenclature. Because this gene locus is amplified in squamous cell carcinoma, we renamed the gene *AIS,* with further designations of splice variants as listed above based on their predicted molecular weight. Note that p68^{AIS} (p73L) described here is ΔNp63α/CUSP and not p73 encoded on chromosome 1.

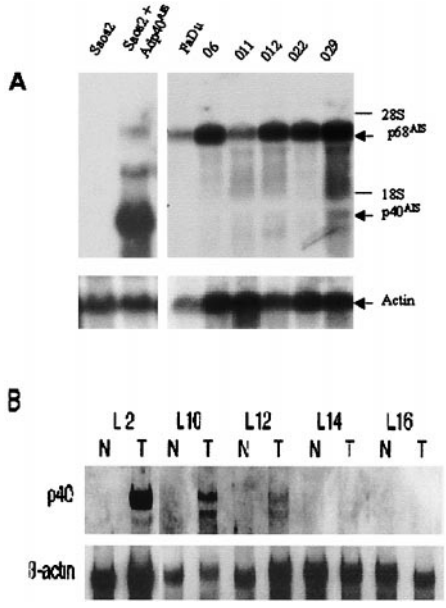

Fig. 2. Detection of *AIS* expression by Northern analysis. (*A*) *AIS* transcripts in HNSCC cell lines and lung cancer cell lines. *AIS* expression is observed in all HNSCC cell lines, whereas no expression is observed in the SaOs2 cell line. A human β-actin probe was used as an internal control. (*B*) Samples (10 μg) of total RNA extracted from tumor (T) and normal (N) tissues of five different patients with primary lung cancers were hybridized with a ^{32}P-labeled probe for *AIS* or β-actin. *AIS* expression of various intensities is observed in the tumor RNA of patients L2, L10, and L12 but is absent from all normal tissue controls.

normal DNA was not available to confirm the somatic origin of these alterations, the conserved nature of these missense variants suggested that inactivation of the gene locus in these human cancers is not common.

Because of its structural similarity to *p53*, we next examined whether *AIS* demonstrated tumor-suppressive effects when constitutively expressed in cultured cells. SaOs2 cells, which have no expression of *p53* (*p53* $-/-$), and *AIS* (null by RT-PCR) were infected with either a replication-incompetent adenovirus containing p40^{AIS} under the control of the cytomegalovirus promoter or a empty adenovirus [multiplicity of infection (MOI) = 3]. Cell numbers were determined on days 1, 3, 5, and 7 after infection. Although the p40^{AIS} adenovirus-infected cells demonstrated abundant p40^{AIS} protein, there was no difference in cell number or viability compared with the control (data not shown). In contrast, SaOs2 cells infected with a *p53* adenovirus showed rapid cell death within 48 h of infection. Overall, these results provided no evidence for a tumor suppressor gene function for variants lacking the N-terminal transactivation domain.

We then examined *AIS* expression in primary lung cancers and HNSCC cell lines by Northern analysis. We found that 10 of 14 primary lung cancers (71%) and all 6 HNSCC cell lines (100%) had an overexpressed message with the AIS probe, whereas normal paired lung tissue and a normal embryonic lung cell line revealed virtual absence of gene expression (Fig. 1; Fig. 2). To explore the possibility that this overexpression was a result of gene amplification, we performed FISH analysis in these tumors (Fig. 3). FISH analysis demonstrated 2- to 5-fold amplification of the *AIS* gene locus in 12 of 23 primary lung cancers (52%), all 9 primary HNSCC (100%), and all 6 HNSCC cell lines (100%) (Table 1). In some cases, a concordant increase in chromosomal arm 3q with a centromeric probe was also observed, confirming the presence of polysomy. The amplification data from FISH analysis correlated with the expression data from Northern analysis in all of the 6 HNSCC cell lines and the squamous cell lung cancers (see below).

Because of the multiple transcripts derived from the same locus, we tested for AIS protein (p40^{AIS} and p68^{AIS}) expression in primary lung cancers, HNSCC cell lines, and primary HNSCC by using immunohistochemistry. To address the specificity of our antibody, Western blot analysis was performed with lysates from SaOs2 (negative for all *AIS* transcripts by RT-PCR), SaOs2 transfected with a p40^{AIS} adenovirus, and the *AIS*-amplified HNSCC cell line (022). We were able to identify a specific band at approximately 40 kDa in the SaOs2 cell line infected with the p40^{AIS} adenovirus and a band at approximately 70 kDa corresponding to p68^{AIS} (or ΔNp63α) in the 022 cell line (Fig. 4*A*). A similar 68-kDa protein was detected in other HNSCC cell lines (Fig. 4*B*). We then probed the Western blots with commercial antibodies specific to the TA domain and the α and γ C terminals. Only the p68^{AIS} product with the α C terminal was consistently overexpressed in the cell lines (data not shown). Some of the cell lines (011, 012, 029) also had low levels of TA-AIS isoforms (data not shown).

By immunohistochemistry, 10 of 23 primary lung cancers (43%), 6 HNSCC cell lines (100%), and all 9 primary HNSCC (100%) had strong positive staining with our polyclonal anti-

Table 1. AIS status in primary lung cancers, HNSCC cell lines, and primary HNSCC

Sample	Sequence variants	Expression (Northern blot)	Immunohistochemistry	Increased copy number	Total
Primary lung cancer					
Total RNA	1/14 (7%)	10/14 (71%)	—	—	14
Sections	—	—	10/23 (43%)	12/23 (52%)	23
HNSCC cell line	1/6 (17%)	6/6 (100%)	6/6 (100%)	6/6 (100%)	6
Primary HNSCC	—	—	9/9 (100%)	9/9 (100%)	9

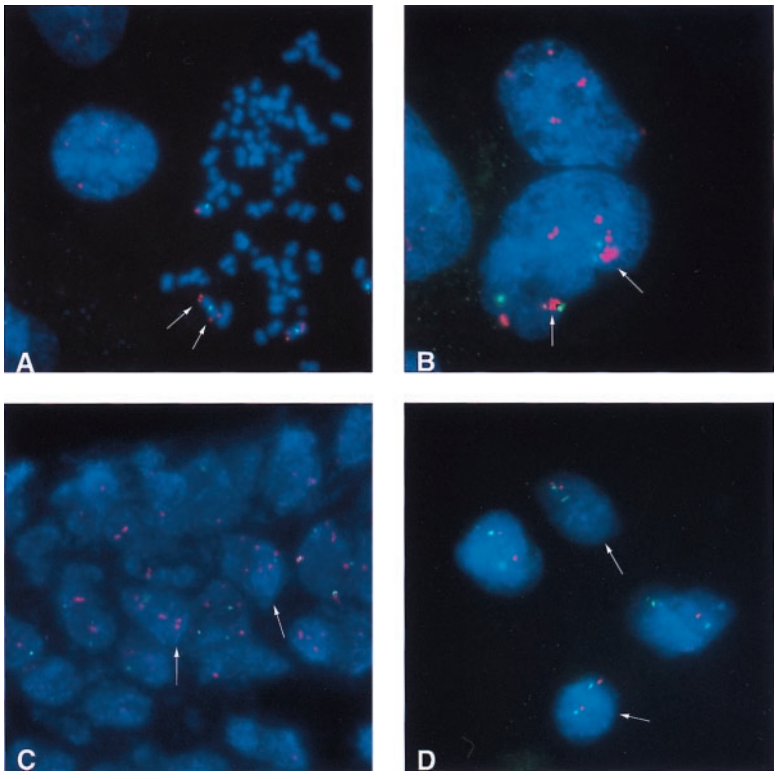

Fig. 3. Detection of *AIS* gene amplification by FISH analysis. (*A*) Low *AIS* gene amplification [bacterial artificial chromosome (BAC) probe, red] was observed on metaphase and interphase nuclei of the HNSCC cell line (FaDu) compared with a chromosome 3 centromeric probe (green). FaDu is known to have an abnormal chromosome 3 karyotype; der(3)t(3:8)(q21:q?). Six signals from the BAC probe were seen on the telomeric end of the long arm of chromosome 3 and on the short arm of chromosome 3 compared with four signals from the chromosome 3 centromeric probe. As a control, normal lymphocytes were subjected to the same FISH analysis to confirm that the BAC probe had no cross-hybridization with other chromosomal regions. (*B*) High *AIS* gene amplification (red, 5-fold) was observed on interphase nuclei of the HNSCC cell line 011 compared with a chromosome 3 centromeric probe (green). (C) A primary squamous cell lung carcinoma (T21) showing two centromeric signals (green) and six to eight *AIS* signals (red) per tumor cell. The number of signals in each cell may vary depending on the focus of the microscope. (*D*) Control hybridization on isolated nuclei preparation from normal bronchial epithelium showing most of the cells with two signals of both chromosome 3 (green) and *AIS* signals (red) (arrows).

body, consistent with $p68^{AIS}$ protein overexpression observed in cell lines (Fig. 5) (Table 1). As shown previously, nuclear staining was present at the basal layer of the bronchial epithelium (9). Nuclear expression was characteristic of those cancers with increased protein. Interestingly, all of the positive samples were squamous cell carcinomas and all had chromosome 3 polysomy or more specific *AIS* amplification (Table 2). In contrast, no adenocarcinomas of the lung had protein overexpression ($P < 0.0001$, Fisher's exact test), suggesting that *AIS* amplifi-

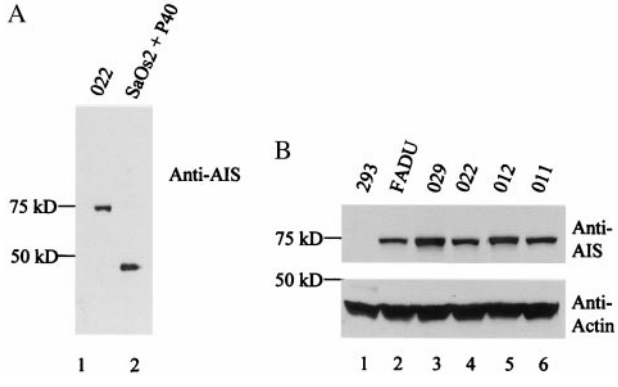

Fig. 4. Expression of *AIS* in HNSCC cell lines. One hundred micrograms of protein extract was subjected to SDS/10% PAGE followed by Western blot analysis as described (12). The antibodies used for probing the blots are indicated on the right and the molecular mass markers are indicated on the left sides of the gels. (*A*) Western blot analysis of HNSCC cell line 022 (lane 1) and SaOs2 cell line expressing $p68^{AIS}$ and $p40^{AIS}$, respectively (lane 2). (*B*) Western blot analysis of various HNSCC cell lines. Lanes: 1, 293; 2, FaDu; 3, 029; 4, 022; 5, 012; and 6, 011. A specific band below 75 kDa is observed in all HNSCC cell lines.

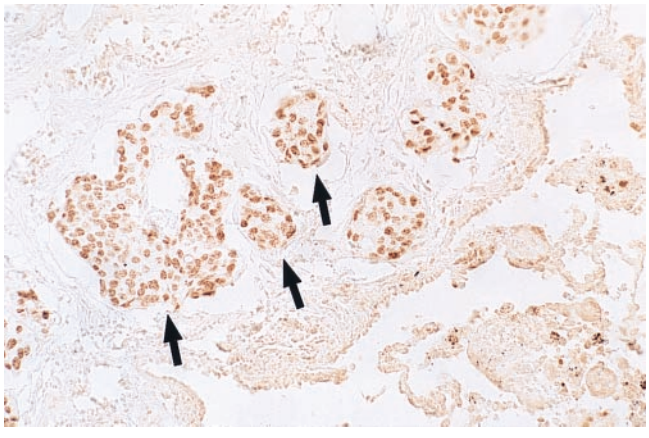

Fig. 5 AIS protein immunoreactivity in squamous cell carcinoma of the lung (T1). Nests of infiltrating tumor cells demonstrate intense nuclear staining (arrows) after incubation with a polyclonal antibody with absence of expression in surrounding normal cells. This tumor had genomic amplification of *AIS* and a *p53* mutation (Table 2). (×200.)

Table 2. *AIS* and *p53* status in 23 primary lung cancers* and 9 primary HNSCC

Sample	Increased copy number (*AIS*)	Immunohisto-chemistry (*AIS*)	Mutation (*p53*)
Lung squamous cell carcinoma			
L10	+	+	+
T1	+	+	+
T3	+	+	+
T13	+	+	+
T14	+	+	−
T17	+	+	+
T20	+	+	−
T21	+	+	+
T22	+	+	+
T23	+	+	+
Total	10/10 (100%)†	10/10 (100%)†	8/10 (80%)
HNSCC			
223	+	+	
232	+	+	
322	+	+	
591	+	+	
1077	+	+	
1111	+	+	
1170	+	+	
1213	+	+	
1227	+	+	
Total	9/9 (100%)	9/9 (100%)	
Lung adenocarcinoma			
L2	+	−	−
L4	−	−	−
L6	−	−	−
L12	+	−	+
L14	−	−	−
L16	−	−	−
T24	−	−	−
T25	−	−	+
T26	−	−	+
T29	−	−	+
T31	−	−	−
T34	−	−	−
T35	−	−	−
Total	2/13 (15%)	0/13 (0%)	4/13 (31%)

*Five primary lung cancers only had total RNA available for analysis.
†$P < 0.0001$ (Fisher's exact test for squamous cell carcinoma vs. adenocarcinoma).

cation correlates with abundant protein only in squamous cell carcinoma.

To examine a possible relationship between *AIS* gene amplification and *p53* status, we proceeded with sequence analysis of the *p53* gene (exons 5 to 8) in the primary lung cancers. Remarkably, 8 of 10 primary lung cancers with $p68^{AIS}$ protein overexpression (80%) also harbored *p53* mutations. (Table 2). This association suggested a possible relationship between overexpression of *AIS* and *p53* inactivation in human cancers.

Table 3. $p40^{AIS}$ enhances colony growth in Rat 1a cells

Cells	No. of colonies 200–400 μm	No. of colonies >400 μm
Rat 1a-$p40^{AIS}$	695 ± 65	37 ± 16
Rat 1a-no	363 ± 125	9 ± 4
P (*t* test)	0.0150	0.0384

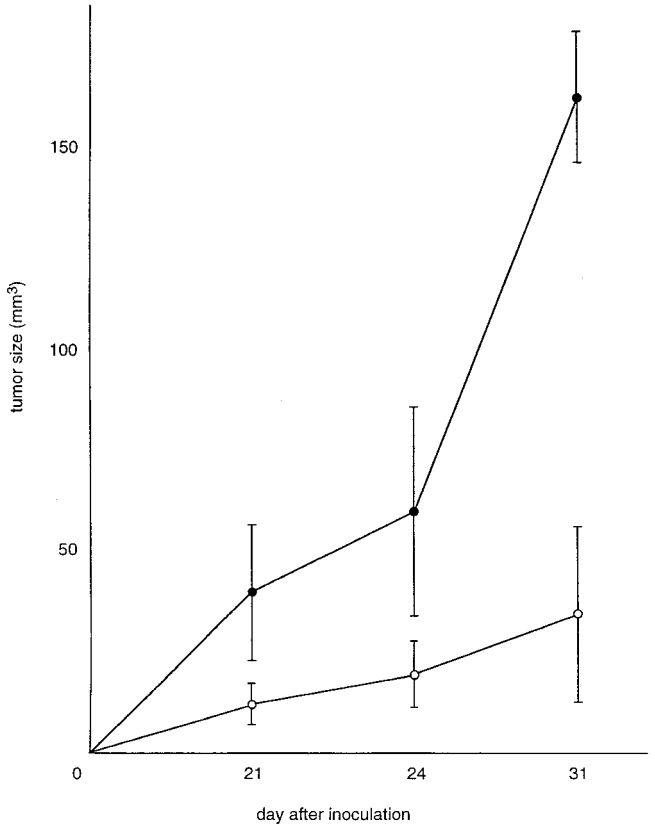

Fig. 6. Tumor growth in nude mice. Rat 1a-$p40^{AIS}$ cells (●) developed into significantly larger tumors compared with Rat 1a-no (○) cells at day 21 ($P = 0.0218$, *t* test), day 24 ($P = 0.0265$), and day 31 ($P < 0.0001$). Each curve represents the mean (±SD) volume of four tumors as shown. On day 31, Rat 1a-$p40^{AIS}$ tumors averaged 162.8 ± 14.8 mm^3, whereas Rat 1a-no tumors averaged 35.0 ± 21.8 mm^3.

The potential oncogenic role of $p40^{AIS}$ was tested in Rat 1a cell clones that overexpressed the protein (Rat 1a-$p40^{AIS}$) or vector only controls (Rat 1a-no). The transformed phenotype of these cell lines was initially assayed by culture in soft agar. Rat 1a-$p40^{AIS}$ cells displayed a significantly increased frequency of colony formation and larger colonies compared with Rat 1a-no cells (Table 3). Pooled clones overexpressing $p40^{AIS}$ were inoculated into nude mice to examine the tumorigenicity of the gene *in vivo*. Tumor size was measured at 21, 24, and 31 days after inoculation, and we found that Rat 1a-$p40^{AIS}$ cells produced significantly larger tumors compared with Rat 1a-no cells (Fig. 6). These observations suggest that AIS overexpression results in an increased tumorigenic phenotype and further support its role as an oncogene.

Discussion

Despite the initial enthusiasm surrounding the cloning of a family of *p53* homologues, there has been little evidence to date as to the role of these genes in the development of human cancers. A role for *p73* (1p36) in c-*abl*-mediated apoptosis was recently proposed (15). Abnormal expression of *p73* has been seen in certain cancers but has been disputed by others (16, 17). Although AIS 3q27 splice variants with a TA domain have been shown to be growth suppressive (8), the most commonly occurring isoform in normal tissue and tumor cells is $p68^{AIS}$ (18). These observations and our results do not support a tumor-suppressor role for these gene in head and neck and lung cancers.

A recent study confirms an absence of inactivating mutations in a large number of human cancer cell lines (19).

Conversely, our work provides tantalizing evidence that the *AIS* locus may play an oncogenic role in human cancer on the basis of the following observations (*i*) The gene locus is overrepresented or amplified in primary lung cancers and HNSCC cell lines by FISH analysis. (*ii*) This increase in copy number is associated with increased expression of RNA by Northern analysis. (*iii*) Increased gene expression is associated with increased protein accumulation as measured by immunohistochemistry in squamous cell cancer. (*iv*) Increased expression of AIS in Rat 1a cells leads to a transformed phenotype.

Our data for *AIS* gene amplification are consistent with recent reports indicating the presence of amplification of chromosomal arm 3q in squamous cell lung carcinoma. Comparative genomic hybridization (CGH) studies indicate that squamous cell lung carcinomas commonly display overrepresentation of the distal arm of chromosome 3q (20). In one study, two candidate genes, *BCHE* and *SLC2A2*, were identified as possible oncogenes because of overexpression in 40% of squamous cell lung carcinomas (21). We have demonstrated consistent overexpression of AIS at the RNA and protein level in those squamous cell carcinomas with an increase in gene copy number. This combined evidence strongly suggests a role for AIS in the progression of these cancers.

Further support for the oncogenic role of AIS protein products comes from our functional assays. Because the locus contains several variants lacking the TA domain with alternate 3′ ends (Fig. 1) we used the core domain $p40^{AIS}$ in our functional studies. Overexpression of $p40^{AIS}$ in Rat 1a cells led to a significant increase in the number and size of colonies in soft agar consistent with previous results in *bona fide* oncogenes (22, 23). Although $p68^{AIS}$ is the predominantly overexpressed isoform in human tumors, the ability of these $p40^{AIS}$-overexpressing cells to form larger tumors in nude mice supports the idea that *AIS* overexpression provides a growth advantage to tumor cells *in vivo*. Because of the high frequency (60%) of amplification and overexpression in lung and head and neck cancer, *AIS* activation may represent one of the most common oncogenic events in human cancer. Other oncogenes such as K-*ras* or cyclin D1 are activated or amplified much less frequently in these cancers (24, 25). One recent study also suggests that $p68^{AIS}$ overexpression is also common in squamous cell carcinoma of the cervix (26).

Although *p73* (located on chromosome 1p) and some splice variants of *AIS* contain a putative transactivating domain capable of inducing apoptosis and tumor suppression, there has been little evidence of inactivating point mutations or other evidence of gene inactivation in human tumors (4, 6, 19). It appears that AIS protein products lacking the acidic N-terminal domain can act in a dominant-negative fashion to diminish transactivation by *p53*. This led to the initial thought that one of these variants may behave as an oncogene in this context by interfering with *p53* function in a competitive manner (9). However, our work suggests that at least in squamous cell cancer, *p53* mutations and *AIS* overexpression commonly occur together. Work in progress suggests a direct protein–protein interaction between $p40^{AIS}$ and wild-type p53 and probably explains the diminution of p53 transactivation in these assays (9). However, it is quite possible that $p40^{AIS}$ may have a gain-of-function phenotype over and above a dominant-negative interaction with p53. Further work will help to elucidate the oncogenic function of AIS in the progression of human cancer.

Two recent reports describe knockout of the *AIS* locus (and all of the transcribed variants) in mice and intriguing developmental defects (27, 28). The skin of these deficient mice does not progress past an early stage in ectodermal development. Moreover, the embryonic epidermis of these knockout mice undergoes an unusual process of nonregenerative differentiation leading to complete absence of all squamous epithelia. The *AIS* locus may thus be critical for progenitor cell populations to maintain continued epithelial development. Overexpression of *AIS* may lead to an increased capacity for epithelial stem cell renewal and the capacity for neoplastic growth. Our data further support the idea that *AIS* amplification and $p68^{AIS}$ overexpression may play a role in the development of squamous cell carcinoma. Moreover, *p53* and *AIS* alterations commonly occur together, suggesting that *AIS* amplification may result in a *p53*-independent pathway of squamous cell carcinoma transformation.

We thank Dr. Bert Vogelstein for various plasmids and critical review of this manuscript. We thank Dr. Christopher Lengauer for critical assessment of the FISH analysis and Robin Lin Brewster for assisting with the preparation of this manuscript. This work was supported by Lung Specialized Programs of Research Excellence Grant CA-5814–02 from the National Cancer Institute and Grant R01 DE-CA1356–01 from the National Institute of Dental and Craniofacial Research. O.L.C. is supported by the Fundação de Amparo à Pesquisa do Estado de São Paulo, Brazil (1998/2736-2).

1. Hollstein, M., Sidransky, D., Vogelstein, B. & Harris, C. (1991) *Science* **253,** 49–53.
2. Sidransky, D., Frost, P., Von Eschenbach, A., Oyasu, R., Preisinger, A. C. & Vogelstein, B. (1992) *New Engl. J. Med.* **326,** 737–740.
3. Mao, L. & Sidransky, D. (1994) *Hum. Mol. Genet.* **3,** 521.
4. Kaghad, M., Bonnet, H., Yang, A., Creancier, L., Biscan, J.-C., Valent, A., Minty, A., Chalon, P., Lelias, J.-M., Dumont, X., *et al.* (1997) *Cell* **90,** 809–819.
5. Gong, J. G., Costanzo, A., Yang, H. Q., Melino, G., Kaelin, W. G., Jr., Levrero, M. & Wang, J. Y. (1999) *Nature (London)* **399,** 806–809.
6. Nomoto, S., Haruki, N., Kondo, M., Konishi, H., Takahashi, T., Takahashi, T. & Takahashi, T. (1998) *Cancer Res.* **58,** 1380–1383.
7. Trink, B., Okami, K., Wu, L., Sriuranpong, V., Jen, J. & Sidransky, D. (1998) *Nat. Med.* **4,** 747–748.
8. Osada, M., Ohba, M., Kawahara, C., Ishioka, C., Kanamaru, R., Katoh, I., Ikawa, I., Nimura, Y., Nakagawara, A., Obunata, M. & Ikawa, S. (1998) *Nat. Med.* **4,** 839–843.
9. Yang, A., Kaghad, M., Wang, Y., Gillett, E., Fleming, M. D., Dotsch, V., Andrews, N. C., Caput, D. & McKeon, F. (1998) *Mol. Cell* **2,** 305–316.
10. Senoo, M., Seki, N., Ohira, M., Sugano, S., Watanabe, M., Tachibana, M., Tanaka, T., Shinkai, Y. & Kato, H. (1998) *Biochem. Biophys. Res. Commun.* **248,** 603–607.
11. Hibi, K., Robinson, C. R., Booker, S., Wu, L., Hamilton, S. R., Sidransky, D. & Jen, J. (1998) *Cancer Res.* **58,** 1405–1407.
12. He, T.-C., Zhou, S., da Costa, L. T., Yu, J., Kinzler, K. W. & Vogelstein, B. (1998) *Proc. Natl. Acad. Sci. USA* **95,** 2509–2514.
13. Hibi, K., Nakamura, H., Hirai, A., Fujikake, Y., Kasai, Y., Akiyama, S., Ito, K. & Takagi, H. (1996) *Cancer Res.* **56,** 480–482.
14. Okami, K., Cairns, P., Westra, W. H., Linn, J. F., Ahrendt, S. A., Wu, L., Sidransky, D. & Jen, J. (1997) *Int. J. Cancer* **74,** 588–592.
15. Agami, R., Blandino, G., Oren, M. & Shaul, Y. (1999) *Nature (London)* **399,** 809–813.
16. Takahashi, H., Ichinomiya, S., Nimura, Y., Watanabe, M., Furusato, M., Wakui, S., Yatani, R., Aizawa, S. & Nakagawara, A. (1998) *Cancer Res.* **58,** 2076–2077.
17. Mai, M., Yokomizo, A., Qian, C., Yang, P., Tindall, D. J., Smith, D. I. & Liu, W. (1998) *Cancer Res.* **58,** 2347–2349.
18. Parsa, R., Yang, A., McKeon, F. & Green, H. (1999) *J. Invest. Dermatol.* **11,** 1099–1105.
19. Hagiwara, K., McMenamin, M. G., Miura, K. & Harris, C. C. (1999) *Cancer Res.* **59,** 4165–4169.
20. Petersen, I., Bujard, M., Petersen, S., Wolf, G., Goeze, A., Schwendel, A., Langreck, H., Gellert, K., Reichel, M., Just, K., *et al.* (1997) *Cancer Res.* **57,** 2331–2335.
21. Brass, N., Racz, A., Heckel, D., Remberger, K., Sybrecht, G. W. & Meese, E. U. (1997) *Cancer Res.* **57,** 2290–2294.
22. Hoang, A. T., Cohen, K. J., Barrett, J. F., Bergstrom, D. A. & Dang, C. V. (1994) *Proc. Natl. Acad. Sci. USA* **91,** 6875–6879.
23. Lewis, B. C., Shim, H., Li, Q., Wu, C. S., Lee, L. A. Maity, A. & Dang, C. V. (1997) *Mol. Cell. Biol.* **17,** 4967–4978.
24. Shiraishi, M., Noguchi, M., Shimosato, Y. & Sekiya, T. (1989) *Cancer Res.* **49,** 6474–6479.
25. Mishima, T., Dosaka-Akita, H., Kinoshita, I., Hommura, F., Morikawa, T., Katoh, H. & Kawakami, Y. (1999) *Br. J. Cancer* **80,** 1289–1295.
26. Nishi, H., Isaka, K., Sagawa, Y., Usuda, S., Fujito, A., Ito, H., Senoo, M., Kato, H. & Takayama, M. (1999) *Int. J. Oncol.* **15,** 1149–1153.
27. Mills, A. A., Zheng, B., Wang, X.-J., Vogel, H., Roop, D. R. & Bradley, A. (1999) *Nature (London)* **398,** 708–713.
28. Yang, A., Schweitzer, R., Sun, D., Kaghad, M., Walker, N., Bronson, R. T., Tabin, C., Sharpe, A., Caput, D., Crum, C. & McKeon, F. (1999) *Nature (London)* **398,** 714–718.
29. Lee, L. A., Walsh, P., Prater, C. A., Su, L.-J., Marchbank, A., Egbert, T. B., Dellavalle, R. P., Targoff, I. N., Kaufman, K. M., Chorzelski, T. P. & Jablonska, S. (1999) *J. Invest. Dermatol.* **113,** 146–151.